

1 **Detergent headgroups control TolC folding *in vitro***

2

3

4 Ayotunde Paul Ikujuni^{a,*}, S. Jimmy Budiardjo^{b,*} and Joanna S.G. Slusky^{a,b,1}

5

6 ^aDepartment of Molecular Biosciences, The University of Kansas, 1200 Sunnyside Ave,

7

Lawrence, KS 66045

8

^bCenter for Computational Biology, The University of Kansas, 2030 Becker Dr., Lawrence, KS

9

66045-7534

10

11

12

13

14

¹To whom correspondence may be addressed. E-mail: slusky@ku.edu 785-864-6519

15

*These authors contributed equally

16

17 **Abstract**

18 TolC is the trimeric outer membrane component of the efflux pump system in *E. coli*
19 responsible for antibiotic efflux from bacterial cells. Over-expression of efflux pumps has been
20 reported to decrease susceptibility to antibiotics in a variety of bacterial pathogens. Reliable
21 production of membrane proteins allows for the biophysical and structural characterization
22 needed to better understand efflux and for the development of therapeutics. Preparation of
23 recombinant protein for biochemical/structural studies often involves the production of proteins
24 as inclusion body aggregates from which bioactive proteins are recovered. Here we find that the
25 *in vitro* folding of TolC into its functional trimeric state from inclusion bodies is dependent on the
26 headgroup composition of detergent micelles used. Nonionic detergent favors the formation of
27 functional trimeric TolC, whereas zwitterionic detergents induce the formation of a non-native
28 trimeric TolC fold. We also find that nonionic detergents with shorter alkyl lengths facilitate TolC
29 folding. It remains to be seen whether the charges in lipid headgroups have similar effects on
30 membrane insertion and folding in biological systems.

31 **Introduction**

32 The Gram-negative bacterial cell envelope contains a distinctive extra protective layer
33 called the outer membrane. The outer membrane not only acts as a protective layer to the cell
34 but also functions as a selective permeability barrier controlling the transport of molecules in
35 and out of the cell (1,2). The outer membrane of Gram-negative bacteria is an asymmetric
36 bilayer composed of phospholipids in the inner leaflet, lipopolysaccharide in the outer leaflet,
37 and outer membrane proteins (OMPs) spanning the bilayer (3).

38 OMPs are almost exclusively antiparallel beta-barrels. They direct diverse cellular
39 functions including signal transduction, general and substrate-specific transport, and enzymatic
40 catalysis (4). OMPs are synthesized in the cytoplasm and targeted to the Sec translocon; a

41 protein complex that helps to transport OMPs across the inner membrane (5). To traverse the
42 periplasmic space, OMPs are aided by periplasmic chaperones (6-9). The folding of the majority
43 of OMPs requires the BAM machinery which catalyzes insertion into the outer membrane (10-
44 14).

45 For biochemical and structural studies which often require a high concentration of
46 proteins, isolating OMPs from their native environment is extremely labor-intensive. This is
47 because the small volume of the outer membrane results in low-yield protein extraction. When
48 possible, refolding of recombinant protein is preferred.

49 Preparation of recombinant outer membrane protein for biophysical or structural studies
50 often involves production of proteins as inclusion bodies, aggregates of unfolded, misfolded,
51 and partially folded protein, from which bioactive proteins are recovered (15). When the signal
52 sequence is removed, single chain outer membrane proteins are known to fold from solubilized
53 inclusion bodies into membrane mimetics like detergent micelles (16,17) or lipid bilayers
54 (18,19). When refolding, the selection of detergent or lipid is often chosen empirically or involves
55 screening mimetics with various chemical properties to achieve proper folding.

56 Previous studies have shown differential effects of various features of membrane
57 mimetics on protein folding. OMP folding rates increase in lipids that form thinner bilayers
58 (20,21), bilayers of increased curvature (21), and bilayers with heat-shock induced lipid
59 dynamics (22,23).

60 Different types of detergents have been employed in the solubilization of membrane
61 proteins for *in vitro* structural and biophysical studies. Although nonionic detergents are the
62 most commonly used detergent in studying membrane proteins, zwitterionic detergents are also
63 frequently employed. Of the zwitterionic detergents used, LDAO is the most common for
64 biochemical and structural analysis of OMPs (24). OMPs that have been studied with LDAO

65 range from small 8-stranded OMPs, OmpW and Ail (25,26), 12-stranded autotransporter, EstA
66 (27), 14-stranded long-chain fatty acid transporter, FadL (28), 16-stranded OMPs sortase, BamA
67 (29) to the multi-barrel porin, OmpF, with three 16-stranded barrels, (30)

68 Outer membrane efflux pumps present a unique challenge in refolding since they are
69 composed of three separate chains. We recently found that with an additional concentration
70 step, multimeric outer membrane proteins such as TolC can be folded into membrane mimetics
71 like single chain barrels are (31). TolC is an outer membrane protein that serves as a
72 component of the tripartite resistance-nodulation-cell-division (RND) efflux pump in *E. coli*,
73 responsible for the expulsion of toxins, including antibiotics, from bacterial cells (32,33).
74 Tripartite RND efflux pumps are composed of three protein subunits that span the inner and
75 outer membranes – where energy from the proton motive force of the inner membrane pushes
76 small hydrophobic molecules out through the periplasmic adapter protein, and then the outer
77 membrane channel (34). The assembly of these three subunits of this pump facilitates extrusion
78 of antibiotics and other toxins from bacterial cells (35). Expression of the AcrABTolC efflux
79 pump is directly correlated with antibiotic resistance in clinical isolates as well as *in vitro*
80 selected mutants of different bacterial pathogens (36-38).

81 The outer membrane pore of TolC is composed of three identical chains (**Figure 1A**)
82 and the folding of TolC into its native trimeric state is essential for the protein to engage the
83 periplasmic subunit of the efflux pump. Because of the prominent role that TolC plays in efflux
84 pump mediated antibiotic resistance, understanding the factors that promote or inhibit the
85 assembly of functional TolC is important for developing inhibitors of efflux pump assembly.

86 In this study, we use *in vitro* refolding experiments and biophysical and biochemical
87 assays to identify a differential effect of detergent headgroup composition on TolC folding *in*
88 *vitro*. We find that TolC only folds correctly in nonionic detergents and that TolC stability is
89 controlled by the particular nonionic headgroup. In contrast, we find that zwitterionic detergents

90 induce the formation of non-native and non-functional trimeric TolC during *in vitro* refolding from
 91 inclusion bodies.

92 Results

93 Different types of detergents have been employed in the refolding and solubilization of
 94 membrane proteins for *in vitro* structural and functional studies. Although nonionic detergents
 95 like n-dodecyl β -D-maltopyranoside (DDM) are most commonly used detergents for membrane
 96 protein purification and structural studies, zwitterionic detergent, n-dodecyl-N,N-dimethylamine-
 97 N-oxide (LDAO) is among the top six detergents used for membrane protein purification and

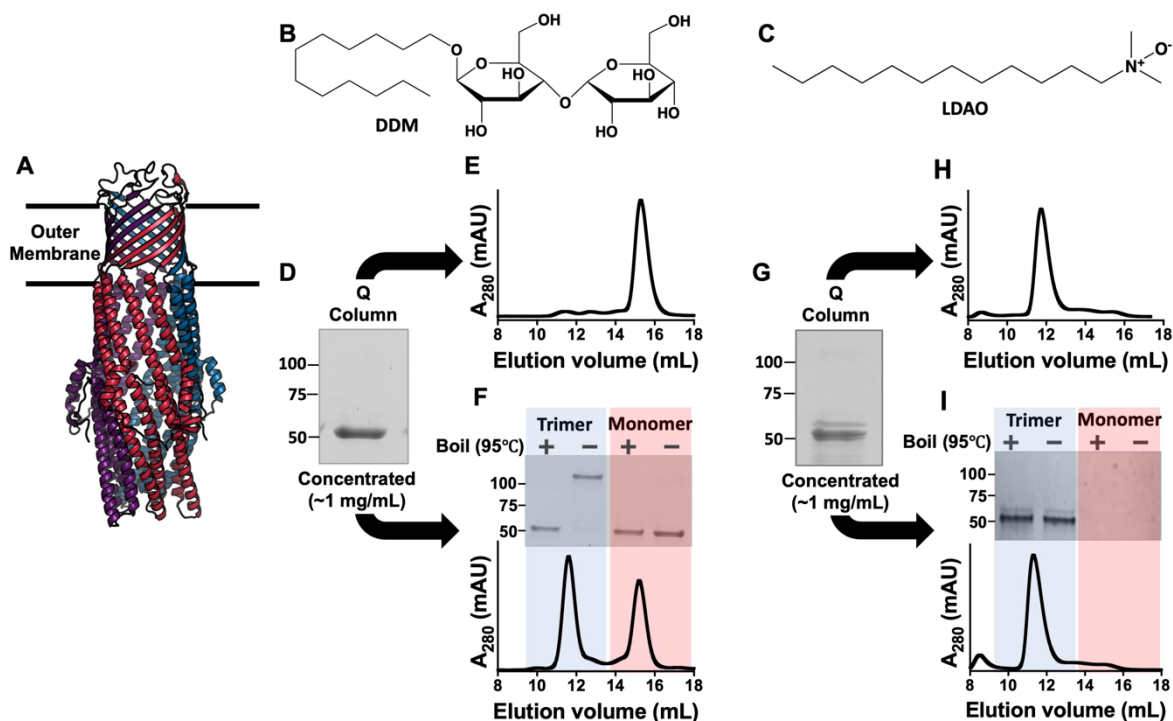


Figure 1: TolC refolded in DDM and LDAO detergents micelles. (A) Structure of trimeric TolC (PDB ID: 1EK9). (B, C) Molecular structure of (A) non-ionic DDM and (B) zwitterionic LDAO. (D) SDS PAGE of TolC in DDM micelles by rapid dilution followed by ion exchange chromatography. (E) SEC chromatogram of TolC elution fraction from ion exchange column in DDM micelles. (F) *Bottom*: SEC chromatogram of concentrated TolC eluate from ion exchange column in DDM micelles. *Top*: SDS PAGE of TolC SEC fractions. (G) SDS PAGE of TolC in LDAO micelles by rapid dilution followed by ion exchange chromatography. (H) SEC chromatogram of TolC elution fraction from Q column in LDAO micelles. (I) *Bottom*: SEC chromatogram of concentrated TolC eluate from ion exchange column in LDAO micelles. *Top*: SDS PAGE of SEC fractions.

98 crystallization (24). Ionic detergents may be more biologically relevant as phospholipids all have
99 at least one negative charge due to the phosphate in their headgroup. In addition the small
100 micellar size of zwitterionic LDAO is reported to be more favorable for protein crystallization
101 (39). DDM is a nonionic detergent with maltose constituting the headgroup and a 12-carbon
102 alkyl group making up the tail (**Figure 1B**). In contrast, LDAO is a zwitterionic detergent with an
103 amine oxide headgroup and a 12-carbon alkyl tail (**Figure 1C**). We have previously reported
104 that *in vitro* refolding of TolC into DDM micelles from inclusion bodies requires three major
105 refolding steps: rapid dilution into detergent micelles, followed by anion exchange
106 chromatography, and then concentration. We found that the third step which involves
107 concentrating the elution fraction from the Q anionic column is essential for the formation of fully
108 folded and functional trimeric TolC (31).

109 Here we find that the choice of detergent can either cause or prevent TolC folding into its
110 native, functional state. TolC from urea-solubilized inclusion bodies was rapidly diluted into
111 detergent and passed through a Q column. When the detergent was DDM, TolC could then be
112 identified by sodium dodecyl sulfate polyacrylamide gel electrophoresis (SDS PAGE) at
113 approximately 51 kDa, corresponding to the size of a single polypeptide chain of TolC (**Figure**
114 **1D**), consistent with previous reports (31,40,41). When this sample is assessed by size
115 exclusion chromatography (SEC), only a peak corresponding to monomeric TolC (about 15 ml)
116 is visible (**Figure 1E**), consistent with previous report (31). When concentrated, TolC trimerizes
117 as indicated by the appearance of a second SEC peak at about 11.5 ml (**Figure 1F Bottom**)
118 and a heat-modifiable, higher molecular weight band on SDS PAGE (**Figure 1F, Top**).

119 In contrast, when TolC from urea-solubilized inclusion bodies was diluted into LDAO, the
120 protein is visible at approximately 51 kDa, corresponding to the size of a single polypeptide
121 chain of TolC, on SDS PAGE (**Figure 1G**), and a peak corresponding to the molecular weight of
122 trimeric TolC (about 11.5 ml) is visible by SEC (**Figure 1H**), consistent with previous reports of

123 SEC chromatogram of trimeric TolC (31,42). Upon subsequent concentration, with TolC in
124 LDAO, we find no significant change in SEC (**Figure 1I, Bottom**) or SDS PAGE (**Figure 1I,**
125 **Top**). This indicates that TolC can form a trimeric species, even in the absence of sample
126 concentration. However, this trimeric species may be more unstable as suggested by the
127 dissociation of the trimer on SDS-PAGE even without boiling (**Figure 1I**).

128 To better distinguish these two seemingly trimeric states of TolC, we used circular
129 dichroism (CD) spectroscopy to quantify the amount of secondary structure formed in the
130 refolded protein. The mean residue ellipticity (MRE) spectrum reveals the presence of
131 secondary structural elements in TolC refolded in both DDM and LDAO micelles (**Figure 2A**).
132 The MRE spectrum of TolC refolded in DDM shows two troughs at about 210 nm and 222 nm
133 and a peak at about 192 nm. For TolC refolded in LDAO micelles, the MRE spectrum showed a
134 significantly shallower trough at about 222 nm compared to DDM micelles consistent with less
135 alpha helical content in LDAO. Furthermore, we observed a shift in the trough from ~210 nm in
136 TolC refolded DDM micelles to ~206 nm in TolC refolded in LDAO micelles, consistent with the
137 presence of more random coil in LDAO micelles. Also, a general decrease in the signal intensity
138 is observed in the CD spectrum of TolC refolded in LDAO micelles compared to DDM micelles
139 (**Figure 2A**). The BeStSel (43) webserver was used to estimate the percentage composition of
140 secondary structural elements in TolC refolded in LDAO micelles compared to DDM micelles.
141 The result indicates that TolC refolded in LDAO is less structured (**Figure 2B**).

142 To further characterize refolded TolC, we examined the unfolding of the protein by
143 monitoring the change in ellipticity at 222 nm as a function of temperature. For TolC refolded in
144 DDM micelles, we observed a progressive shift in MRE at 222 nm as temperature increased
145 beyond 75 °C, indicating protein unfolding due to high temperature. However, we observed no
146 melting point in the CD signal at 222 nm with TolC refolded in LDAO micelles within the

147 temperature range of 20 to 90 °C used in this study (**Figure 2C and S1**). These CD data
 148 suggest that trimeric TolC formed in LDAO micelles has a different conformation and is possibly
 149 less folded than trimeric TolC formed in DDM micelles.

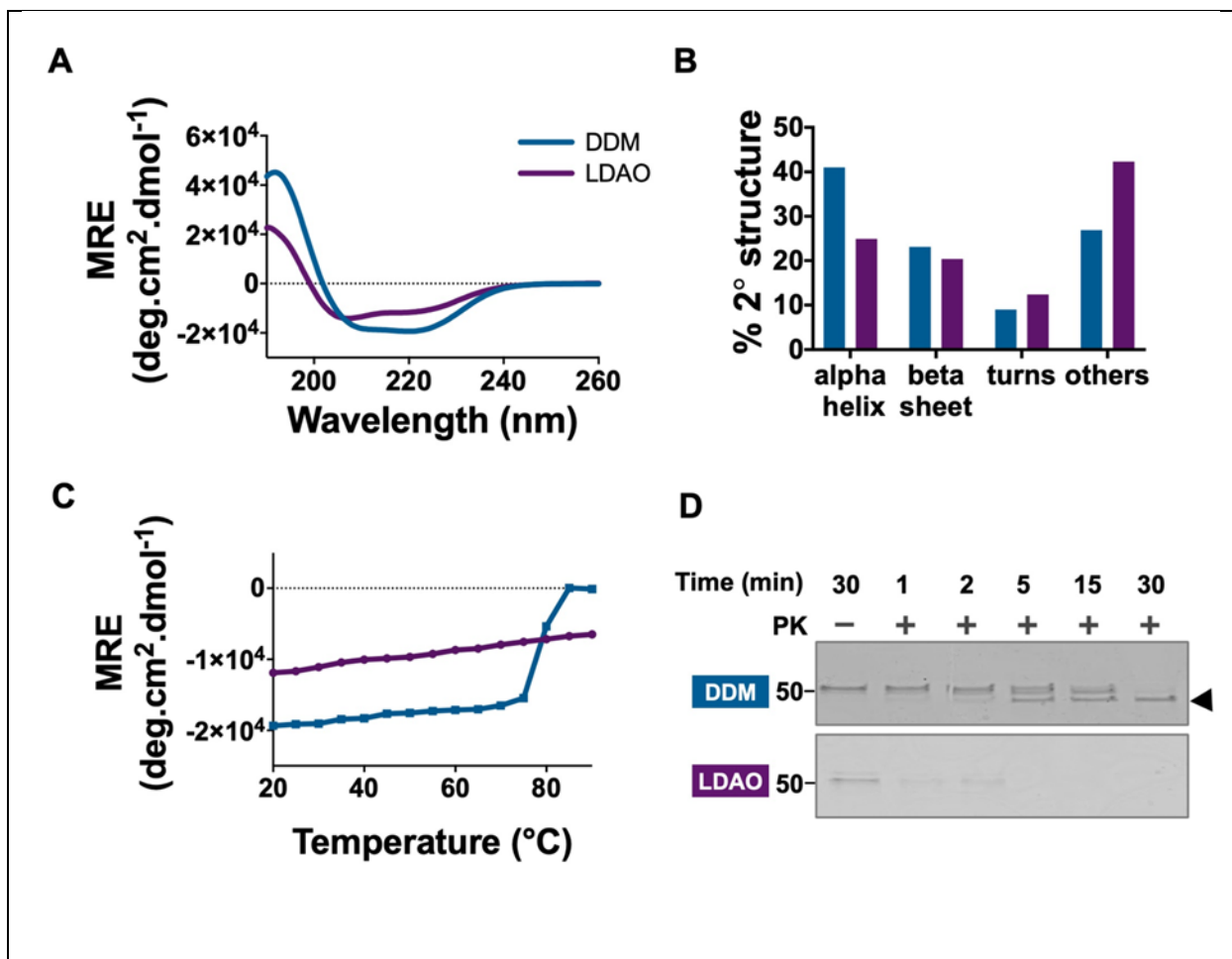


Figure 2: Trimeric TolC is less folded and less inserted in LDAO than in DDM. (A) Overlaid CD spectra of TolC refolded in DDM (blue) and LDAO (purple) micelles. (B) Secondary structure estimation of TolC refolded in DDM (blue) and LDAO (purple) using BeStSel (43) web server. (C) Overlaid mean residue ellipticity (MRE) of TolC refolded in DDM (blue) and LDAO (purple) at 222 nm as a function of temperature. (D) SDS PAGE analysis of trimeric TolC refolded in DDM (blue) and LDAO (purple) incubated with proteinase K. Black arrowhead represents proteinase K digestion resistant product.

150 Based on this observation, we used a proteinase K digestion assay to assess the
 151 conformation of TolC refolded in LDAO micelles. Previous studies have reported that correctly
 152 folded TolC becomes resistant to proteinase K digestion, forming a 46 kDa digestion-resistant

153 product (44,45). Refolded TolC in both DDM and LDAO micelles were subjected to proteinase K
154 digestion. The digestion products were then boiled and visualized by SDS PAGE. TolC refolded
155 in DDM was resistant to proteinase K and formed a 46 kDa digestion resistant product after a 30
156 minutes incubation. However, TolC refolded in LDAO micelles was completely digested by
157 proteinase K within 30 min of incubation (**Figure 2D**).

158 The above data indicate that although TolC refolded in LDAO micelles exists as a trimer,

Table 1: Detergents used to refold TolC in this study.

	Name	Chain length	Headgroup	Headgroup type
DDM	n-dodecyl- β -D-maltopyranoside	12	maltose	Nonionic
OM	n-octyl- β -D-maltopyranoside	8	maltose	Nonionic
C12E8	octaethylene glycol monododecyl ether	12	polyoxyethelene	Nonionic
C8POE	n-octylpolyoxyethylene	8	polyoxyethelene	Nonionic
LDAO	n-Dodecyldodecyl-N,N-dimethylaminedimethylamine-N-Oxide oxide	12	amine oxide	Zwitterionic
SB3-12	sulfobetaine 3-12 (SB3-12)	12	sulfobetaine	Zwitterionic

159 it assumes a different conformation than in DDM micelles. We further sought to understand
160 what property of detergents results in the native-like or non-native-like TolC folding. We
161 screened four additional detergents varying headgroups and alkyl chain lengths and observed
162 their effects on the folding, stability, and function of TolC. These include three nonionic
163 detergents n-octyl- β -D-maltopyranoside (OM), n-octylpolyoxyethylene (C8POE), and
164 octaethylene glycol monododecyl ether (C12E8), and one zwitterionic detergent, sulfobetaine 3-
165 12 (SB3-12) (**Table 1**). Like DDM, C12E8 has a hydrophobic tail with a 12-carbon alkyl group
166 while C8POE and OM have an 8-carbon tail length. The headgroup of DDM and OM is
167 composed of maltose while that of C12E8 and C8POE have polyoxyethylene (**Figure 3A-D**).
168 SB3-12 has a 12-carbon hydrophobic tail length like LDAO, and a positively and negatively
169 charged headgroup contributed by nitrogen and oxygen respectively (**Figure 3D**).

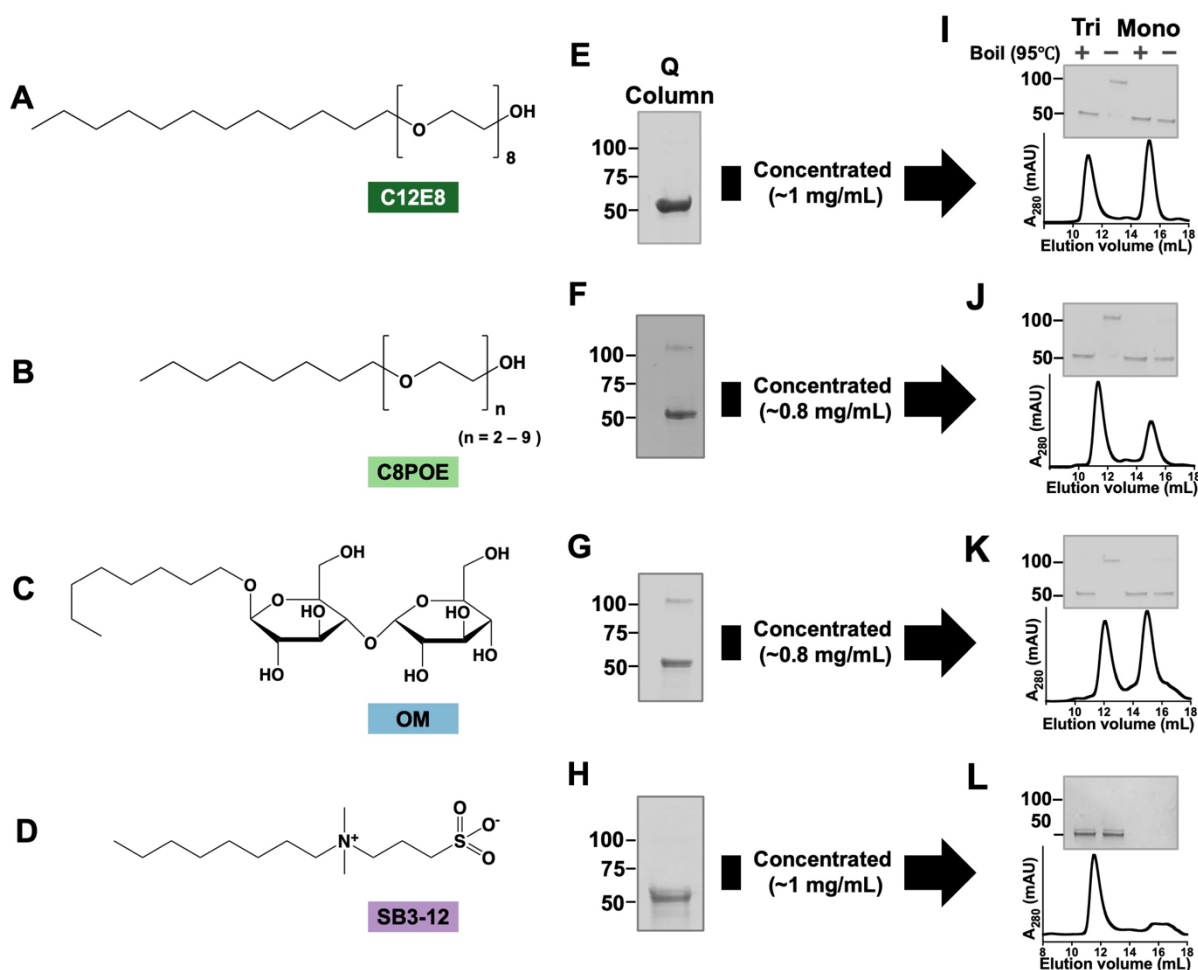


Figure 3: ToIC trimerization before concentration depends on detergent headgroup and alkyl chain length. After concentration, ToIC trimerization is only dependent on detergent headgroup. (A-D) Molecular structures of (A) n-octyl-β-D-maltopyranoside, (B) octaethylene glycol monododecyl ether, (C) sulfobetaine 3-12, (D) n-octylpolyoxyethylene. (E-H) SDS PAGE of ToIC refolded in (E) C12E8, (F) C8POE, (G) OM, and (H) SB3-12 micelles by rapid dilution followed by ion exchange chromatography. (I-L) SDS-PAGE and SEC chromatogram of captured monomeric (right) and trimeric (left) ToIC refolded in (I) C12E8, (J) C8POE, (K) OM, and (L) SB3-12.

170 Using an identical protocol to previous ToIC folding, urea-solubilized inclusion bodies
 171 were rapidly diluted into detergent and then passed through a Q-column. ToIC diluted into
 172 C12E8 and SB3-12 and visualized on SDS-PAGE, resolved at a molecular weight
 173 corresponding to the size of monomeric ToIC (**Figure 3E and 3H**). However, SDS PAGE shows
 174 that ToIC trimerizes more readily in detergent micelles with shorter alkyl chain length C8POE,
 175 and OM than longer chain length, DDM and C12E8. (**Figure 3F-G**). However, when

176 concentrated, only the detergents with nonionic head groups developed the trimer band
177 visualized by SDS PAGE which is confirmed with a concomitant trimeric peak on SEC (**Figure**
178 **3I, 3J and 3K**). In contrast, in the zwitterionic SB3-12 detergent micelles, we saw a similar trend
179 observed with zwitterionic LDAO micelles where refolded TolC elutes at a volume
180 corresponding to the size of trimeric TolC on SEC but resolves at a size corresponding to
181 monomeric TolC on SDS PAGE (**Figure 3L**).

182 We used CD to investigate the folding of TolC in each of the detergents tested. We observed
183 overlapping CD spectra of trimeric TolC refolded in all the nonionic detergents tested (**Figure 4A**)
184 indicating a similar level of secondary structure formation. In the same way, TolC refolded in
185 zwitterionic SB3-12 has a similar CD spectrum to TolC refolded in zwitterionic LDAO (**Figure**
186 **4A**). Consistent with TolC refolded into zwitterionic LDAO, TolC refolded into zwitterionic SB3-
187 12, shows no melting point in the temperature range used in this study (**Figure 4B and S1**).

188 In addition to the differences in the folding in nonionic and zwitterionic detergents, the
189 thermal denaturation assay reveals another head group-based difference in the thermodynamic
190 stability of TolC within the nonionic detergents. Though TolC folded in nonionic detergents
191 demonstrates heat modifiability on SDS-PAGE and has a similar secondary structure as
192 measured by CD, TolC is substantially more stable in the maltose-headgroup lipids. The T_m of
193 TolC in the maltose headgroup detergents is 30 – 40 °C higher than the T_m of TolC in
194 polyoxyethylene headgroup detergents (**Figure 4B and S1**).

195 While trimers form even without concentration for either nonionic eight-carbon chain
196 lipid, the effect of chain length on the stability of TolC in the tested nonionic detergents differs
197 depending on the headgroup composition. For detergents with maltose head group, the 12-
198 carbon length chain increased the T_m about 7 °C more than the 8 carbon length. Conversely,
199 while for detergents with polyoxyethylene headgroup, the 8 carbon length chain increased the
200 T_m about 3 °C more than the 12 carbon.

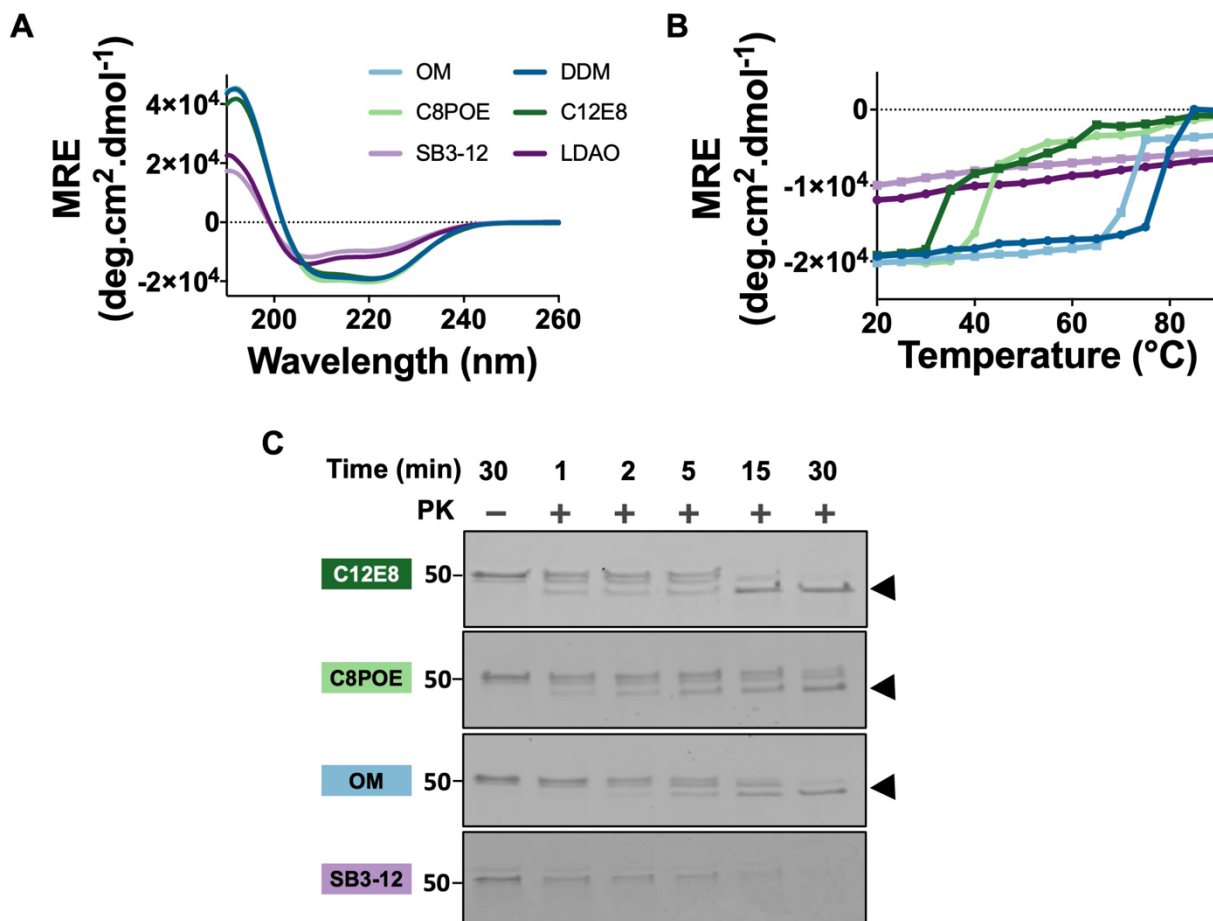


Figure 4: Secondary structure and PK resistance of TolC is dependent on detergent headgroup and not alkyl chain length. (A) Overlaid CD spectra of DDM (dark blue), OM (light blue), C8POE (light green), C12E8 (dark green), LDAO (dark purple), and SB312 (light purple). (B) MRE of TolC at 222 nm as a function of temperature. (C) SDS PAGE analysis of trimeric TolC incubated with proteinase K in detergents.

201 The observed variance in the stability of TolC in the different detergents tested, led us to
 202 investigate the conformation of TolC and its insertion into the tested micelles by PK digestion
 203 assay. The PK digestion assay indicates that, like nonionic DDM, trimeric TolC refolded in all
 204 nonionic detergents—C12E8, OM, and C8POE—is resistant to proteinase K digestion and
 205 forms a 46 kDa digestion resistant product. However, like zwitterionic LDAO, TolC refolded in
 206 zwitterionic SB3-12 detergent micelles was completely digested within 30 min of incubation with
 207 PK (**Figure 4C**). This indicates that in all nonionic detergents we tested, TolC is in a native-like

208 conformation, but that in all zwitterionic detergents we tested, ToIC is in a non-native
209 conformation.

210 Because the melting temperature data and proteinase K digestion data indicate a
211 possible difference in conformation between ToIC folded in nonionic detergents and ToIC folded
212 in ionic detergents, we sought to determine if ToIC refolded in zwitterionic detergents (LDAO
213 and SB3-12) can bind native ToIC ligand colicin E1 (46,47). Using a coelution assay, a mixture
214 of refolded ToIC and ColE1 was incubated for an hour and then separated on an SEC column.
215 We observed a shift in the elution peak in the SEC chromatogram of the mixture of ColE1 and
216 ToIC refolded in all of the four nonionic detergents tested when compared with that of ToIC
217 alone. This elution peak shift indicates the presence of a ToIC-ColE1 adduct formed from the
218 interaction of ToIC with ColE1 (**Figure 5A-D**). However, the SEC chromatogram shows no shift

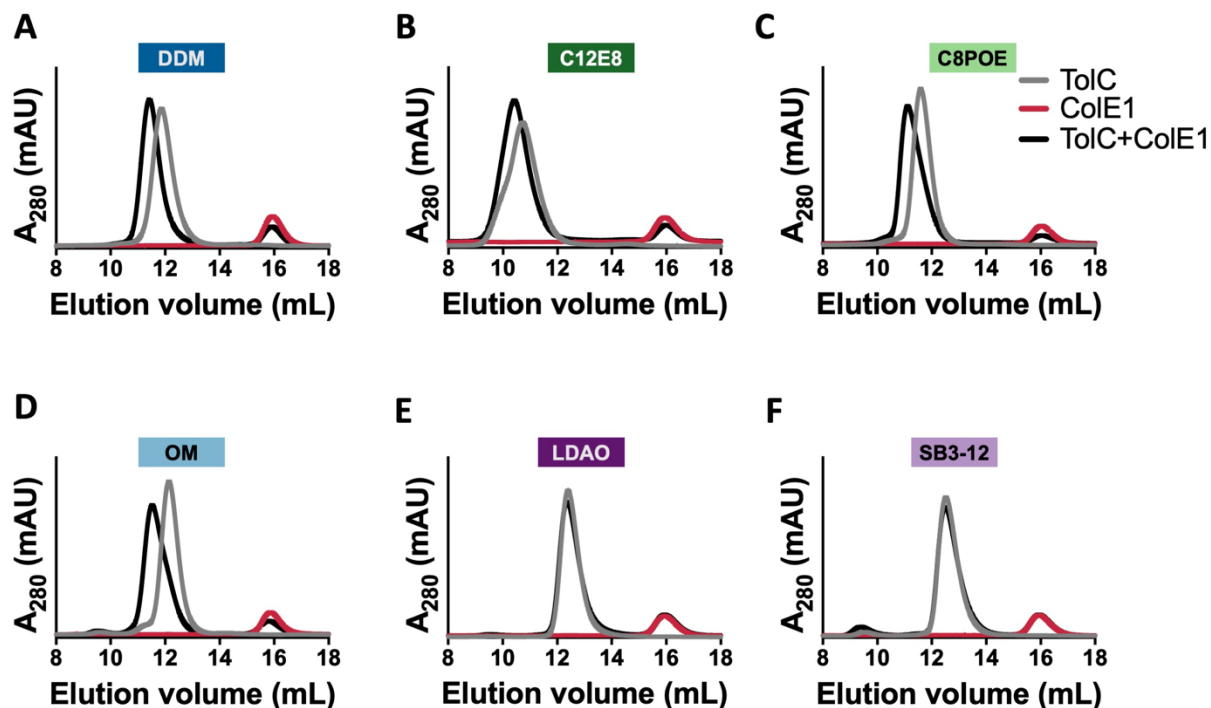


Figure 5: Effect of detergent headgroup on ToIC binding to a native ligand. SEC chromatograms of ColE1 (red), ToIC+ColE1 (black) with ToIC refolded in (A) DDM, (B) C12E8, (C) C8POE, (D) OM, (E) LDAO, and (F) SB3-12. 10 μ M of ToIC was incubated with 20 μ M of ColE1.

219 in the elution volume when ColE1 is mixed with trimeric TolC refolded in LDAO or SB3-12
220 micelles. (**Figure 5 F-G**). Therefore, although TolC forms a monodispersed trimer when refolded
221 in zwitterionic detergent micelles, the trimer formed has a different conformation from native
222 TolC and does not bind to its endogenous binding partner.

223 Discussion

224 TolC exists in its native and functional state in the outer membrane as a trimer with each
225 polypeptide chain contributing to the formation of a cylindrical, β -barrel crowning an α -helical
226 barrel (45,48,49). This conformation is essential for TolC to perform its function in the outer
227 membrane.

228 It has only recently been determined that TolC can be folded *in vitro* (31). Here we find a
229 different TolC folding behavior in zwitterionic detergent micelles compared to nonionic detergent
230 micelles. Although refolded TolC forms a monodispersed trimer in zwitterionic detergent
231 micelles as observed in the SEC chromatogram (**Figure 1G**), we find that this is not the native
232 conformation. Structural (**Figure 4**) and functional (**Figure 5**) characterization show that trimeric
233 TolC formed in zwitterionic detergent micelles has a different conformation than native trimeric
234 TolC. Although we may have expected the soluble, periplasmic α -helical portion to form
235 regardless of the detergent used, we find instead that TolC in zwitterionic micelles have half the
236 α -helical content but comparable β -sheet content.

237 Previous studies have indicated that *in vitro* OMP folding involves the formation of an
238 intermediate step where OMPs associate with the membrane mimetics before they are inserted
239 into the micelles or bilayers (50). The hydrophilic, periplasmic α helix domain of TolC is
240 composed of clusters of charged residues. We speculate that the non-native folded state we
241 observed in zwitterionic detergent micelles may be a low-energy state formed by interactions
242 between residues of the α helix domain of TolC and the charged headgroup of the

243 zwitterionic detergent micelles. If that were the case, charge-charge interactions would lead to
244 the formation of non-native, stable, but non-functional trimeric TolC on the surface of the
245 detergent micelle.

246 Our finding that more trimer is visible by SDS page when diluting into detergent micelles
247 with shorter acyl chains before concentration (**Figure 3**) is in agreement with previous studies
248 that showed single-chain OMPs fold more readily into lipids with shorter hydrocarbon chains
249 (20,21,23).

250 Both the polyoxyethylene detergent micelles and maltoside detergent micelles remain
251 intact upon heating until well above the TolC unfolding transitions (51-53). Since the unfolding is
252 not due to de-micellation, the unfolding temperature is likely a property of the TolC interaction
253 with the headgroup rather than a property of the micelle itself. Maltose headgroup detergents
254 (DDM and OM) stabilize the TolC trimer at higher temperatures. TolC denaturation in maltoside
255 detergents takes place over a narrow temperature range, starting at about 70 °C to 75 °C and
256 complete denaturation is observed at about 75 °C to 80 °C (**Figure 4B, Figure S1**). The spectra
257 of the semi-denatured state appear more like an alpha helix before complete denaturation
258 (**Figure S1**). However, native-like trimeric TolC is substantially less stable in detergent with
259 polyoxyethylene headgroups (C12E8 and C8POE). For polyoxyethylene headgroup detergents,
260 TolC denaturation starts at about 40 °C and a gradual loss of secondary structure is observed
261 until complete denaturation is reached at about 65 °C. Moreover, as denaturation begins, the
262 spectra appear more like a beta-sheet before complete denaturation is achieved (**Figure S1**).
263 Thus, the alpha helical part of TolC is possibly disrupted by polyoxyethylene headgroups.

264 Consistent with previous reports for other OMPs (20,21), we find that shorter alkyl chains
265 facilitate TolC insertion even without concentration. However, we find different effects of chain
266 length on stability depending on the headgroup. Polyoxyethylene increases stability for shorter
267 alkyl chains and maltose headgroups decreasing stability for shorter alkyl chains. Consistent

268 with our temperature melt data, perhaps the long polar region of the oxyethylene headgroups
269 disrupts the helical region of TolC with the longer eight oxyethylene disrupting more than POE
270 which has a distribution of two to nine oxyethylene. This is consistent with small amounts of
271 beta structure remaining in the unfolded state of TolC folded in polyoxyethylene micelles
272 (**Figure S1**). When there are no oxyethylene present TolC is more stable in the longer (C12)
273 alkyl chain of DDM than the shorter (C8) alkyl chain of OM.

274 Finally, we anticipate that our data will help to better understand the biogenesis of outer
275 membrane efflux pumps. Overall, we find that the head group composition of detergents plays a
276 significant role in the folding of multimeric outer membrane efflux pumps *in vitro*, with
277 zwitterionic lipids preventing TolC folding. These findings may contribute answers to long-
278 standing questions of OMP folding: 1) Why can we so easily refold OMPs *in vitro* but *in vivo*
279 folding requires the BAM complex and 2) Once proto-OMPs are in the periplasm, how does
280 nature prevent OMP folding back into the inner membrane phospholipids. At least for TolC, the
281 answer may be that the natural negative charge of the phosphate in all phospholipids as well as
282 the zwitterionic headgroup of the dominant membrane lipid phosphatidylethanolamine (54)
283 prevents folding into both the outer leaflet of the inner membrane and the inner leaflet of the
284 outer membrane. In contrast, the common laboratory use of non-ionic detergents facilitates TolC
285 folding *in vitro*. It will be important to continue to investigate the biological relevance of this effect
286 and to determine how bacterial cells facilitate efflux pump folding in the presence of zwitterionic
287 lipids.

288 **Materials and Methods**

289 ***E. coli* strains**

290 *E. coli* BL21(DE3) was used for the expression of TolC as inclusion bodies.

291 **Expression and purification of Colicin E1**

292 Colicin E1 was expressed and purified as previously described (47). Briefly, residues 1-190 of
293 colicin E1 (colE1-T) were cloned into pET303 containing a C-terminal 6x histidine tag. Plasmids
294 were transformed into BL21(DE3) and plated on LB + agar + 100 µg/ml carbenicillin. A single
295 colony was inoculated into 20 ml of LB + 100 µg/ml carbenicillin and grown at 37 °C with
296 shaking at 250 rpm overnight. The next morning 1L TB broth + 10 mM MgCl₂ + 100 µg/ml
297 carbenicillin was inoculated with 20 ml of the overnight starter culture and grown at 37 °C with
298 shaking at 250 rpm until OD₆₀₀ reached 1.0 and induced with 1 mM IPTG. The temperature was
299 reduced to 15 °C with shaking at 250 rpm and incubated for 24 hours. Cell pellets were
300 harvested by centrifugation at 4,000 g for 30 minutes at 4 °C. Cell pellets were resuspended in
301 lysis buffer (TBS, 5 mM MgCl₂, 0.2 mg/ml lysozyme, 5 µg/ml DNase, 1mM PMSF, 20 mM
302 imidazole) at 3 ml/g of cell pellet. Cells were lysed by sonication in an iced water bath (3 min, 2
303 sec on, 8 sec off, 40 % amplitude, QSonica Q500 with 12.7 mm probe). The cytoplasmic
304 fraction was isolated by centrifugation at 50,400 g at 4 °C for 1 hour. The supernatant was
305 filtered through 0.22 µm membrane filter and applied to a 5 ml HisTrap FF column and purified
306 using an ÄKTA FPLC system with 20 column volumes wash step with binding buffer (20 mM
307 Tris, 40 mM NaCl, 25 mM imidazole) and eluted using a linear gradient from 0 – 100% elution
308 buffer (20 mM Tris, 400 mM NaCl, 500 mM imidazole) in 10 column volumes. Colicin-containing
309 fractions were pooled and concentrated to 2 ml and applied onto a HiLoad 16/60 Superdex 200
310 pg column and eluted with 1.5 column volumes in 20 mM Tris, 40 NaCl.

311 **Expression and purification of TolC as inclusion bodies**

312 TolC was expressed and purified as previously described (31). TolC gene was received from R.
313 Misra and cloned into pTrc99a. The signal sequence was deleted for inclusion bodies
314 expression using the forward primer 5'- CATGGTCTGTTTCCTGTGTGAAATTG -3' and reverse
315 primer 5'- GAGAACCTGATGCAAGTTTATCAGC -3'. A sequence confirmed plasmid of TolC
316 was transformed into *E. coli* BL21(DE3) cells and plated on an LB agar plate with 100 µg/ml of
317 carbenicillin. A single colony from the plate was used to inoculate a 20 ml of LB media
318 containing 100 µg/ml carbenicillin which was then incubated at 37 °C, 250 rpm overnight (~ 16
319 h). This starter culture was used to inoculate 1L of LB media containing 100 µg/ml carbenicillin.
320 The culture was grown at 37 °C, 250 rpm until it had an optical density (OD) at 600 nm of ~0.6.
321 Then expression of TolC was induced with 1 mM of Isopropyl β-D-1-thiogalactopyranoside
322 (IPTG) while the culture remained incubated at 37 °C, 250 rpm for 4 h. Cells were harvested by
323 centrifugation at 4,000 g for 25 min at 4 °C. Cell pellets were resuspended in lysis buffer (TBS, 5
324 mM MgCl₂, 0.2 mg/ml lysozyme, 5 µg/ml DNase, 2 mM phenylmethylsulfonyl fluoride (PMSF), 1
325 % (v/v) Triton X-100) at 3 ml/g of cell pellet and lysed via sonication (3 min, 3 sec on, 7 sec off,
326 40% amplitude, QSonica Q500 with 12.7 mm probe) in an iced water bath. The lysate was
327 centrifuged at 4,000 g for 25 min at 4 °C and the pellet was resuspended in 40 ml wash buffer
328 (TBS, 1% (v/v) Triton X-100). The lysate was sonicated on an ice bath for an additional three
329 minutes and the inclusion bodies were recovered by centrifugation at 4,000 g for 25 min at 4 °C.
330 The inclusion bodies pellet was washed by resuspension in 40 ml wash buffer and centrifuged
331 at 4,000 g at 4 °C for 25 min. The inclusion bodies pellet was then resuspended in 20 mM Tris-
332 HCl, pH 8, aliquoted, and stored at -20 °C until further use.

333 **Refolding TolC**

334 TolC was refolded as previously reported (31). Briefly, inclusion bodies were thawed and
335 centrifuged at 4,000 g for 25 min at 4 °C. The inclusion body pellet was dissolved in urea buffer

336 (20 mM Tris-HCl, pH 8, 8 M urea) and incubated at 37 °C for about 15 min. Solubilized inclusion
337 was then centrifuged at max speed on a table-top centrifuge for 5 min to get rid of insoluble
338 inclusion bodies. To initiate refolding, 4 mg/ml of solubilized TolC inclusion bodies was rapidly
339 diluted by 25-fold into refolding buffer (20 mM Tris-HCl, pH 8.0) containing detergent of interest
340 (0.5 % (w/v) n-dodecyl β -D-maltopyranoside (DDM, Anatrace) or 2 % (w/v) n-Octyl- β -D-
341 maltopyranoside (OM, Anatrace) or 1 % (w/v) n-dodecyl-N,N-dimethylamine-N-Oxide (LDAO,
342 Anatrace) or 1 % (w/v) sulfobetaine 3-12 (SB3-12, Sigma-Aldrich) or 1 % (v/v) n-
343 octylpolyoxyethylene (C8POE, Bachem) or 0.5 % (w/v) octaethylene glycol monododecyl Ether
344 (C12E8, Anatrace) and gently mixed on a rotisserie. The solution was passed through a 0.22
345 μ m membrane filter and loaded onto a 5 ml HiTrap Q HP anion exchange column (GE
346 Healthcare, USA) equilibrated with wash buffer (20 mM Tris-HCl pH 8.0) containing detergent of
347 interest (0.05 % (w/v) DDM or 2 % OM or 0.2 % (w/v) LDAO or 2 % (w/v) SB3-12 or 0.6 % (v/v)
348 C8POE or 0.05 % (w/v) C12E8). The column was then washed with 5 column volumes of wash
349 buffer. The protein was then eluted with 3 column volumes of elution buffer (20 mM potassium
350 phosphate buffer pH 8, 500 mM sodium fluoride) containing the same concentration of
351 detergent of interest in wash buffer. 2X Laemmli SDS sample buffer was added to each sample
352 and loaded on a 4 – 20 % polyacrylamide gel for SDS-PAGE analysis. Gels were imaged with
353 an Epson Perfection V600 photo scanner.

354 **Size exclusion chromatography**

355 Elution fractions from TolC refolding above were pooled and concentrated using an Amicon
356 centrifugal protein concentrator of 10K molecular-weight cutoff at 4,000 g and 4 °C to a
357 concentration of about 1 mg/ml unless otherwise stated. The sample was then filtered with an
358 0.22 μ m filter. 500 μ l of sample was loaded and the loop was emptied with 2.5 ml elution buffer
359 onto a Superdex 200 Increase 10/300 pg size exclusion column, pre-equilibrated with the

360 elution buffer. The sample was then eluted with the elution buffer containing the detergent of
361 interest.

362 **CD spectroscopy**

363 CD spectra were recorded using a J-815 spectrometer (Jasco, Germany) from 260 to 190 nm.
364 Thermal melt spectra were obtained by CD between 20 °C and 90 °C at 0.5 nm intervals in a 0.1
365 cm pathlength quartz cuvette. Spectra were collected at 5 °C temperature interval and 5 °C/min
366 temperature ramp time with two minutes of equilibration time at each target temperature. Two
367 replicates were collected for each protein sample and baseline (elution buffer) at 100 nm/min
368 scanning speed, a digital integration time of two seconds, and a bandwidth of 1.5 nm. The
369 spectra were smoothed with a Savitsky-Golay filter, and the baseline was subtracted from each
370 protein sample. Data were converted to mean residue ellipticity and secondary structure
371 analysis was done using BeStSel web server (43).

372 **Proteinase K digestion**

373 The assembly of refolded TolC was assessed by proteinase K digestion. 15 µg of protein was
374 treated with 15 µg of Proteinase K on ice for 1, 2, 5, 15, and 30 min. 2 mM PMSF was added to
375 inactivate the protease and the reaction was boiled at 95 °C for 5 min. The susceptibility of
376 protein to the proteinase K was determined by SDS PAGE.

377 **Coelution**

378 TolC and Colicin E1 were both buffer exchanged into coelution buffer (20 mM Tris pH 8.0, 40
379 mM NaCl, containing detergent of interest) using PD-10 desalting columns. Binding was
380 determined by coelution on a Superdex 200 Increase 10/300 size exclusion column. 1:2 molar
381 ratio (5 µM TolC trimer to 10 µM ColE1) of TolC and ColE1 respectively were mixed and
382 incubated at room temperature for 1 hour.

383 Acknowledgment

384 We thank Rajeev Misra for the pTrc vector containing TolC gene. We gratefully acknowledge
385 NIGMS awards DP2GM128201 to JS GS, NIGMS awards P20 GM103418 and 2K12GM063651
386 to SJB. We also acknowledge feedback from Rik Dhar, Ryan Feehan, Daniel Montezano, Alex
387 Bowman, and Samuel Lim.

388

389 References:

- 390 1. Nikaido, H. (2003) Molecular Basis of Bacterial Outer Membrane Permeability Revisited.
391 *Microbiology and Molecular Biology Reviews* **67**, 593-656
- 392 2. Zgurskaya, H. I., López, C. A., and Gnanakaran, S. (2015) Permeability barrier of Gram-negative
393 cell envelopes and approaches to bypass it. *ACS infectious diseases* **1**, 512-522
- 394 3. Kamio, Y., and Nikaido, H. (1976) Outer membrane of *Salmonella typhimurium*: accessibility of
395 phospholipid head groups to phospholipase C and cyanogen bromide activated dextran in the
396 external medium. *Biochemistry* **15**, 2561-2570
- 397 4. Koebnik, R., Locher, K. P., and Van Gelder, P. (2000) Structure and function of bacterial outer
398 membrane proteins: barrels in a nutshell. *Molecular microbiology* **37**, 239-253
- 399 5. Brundage, L., Hendrick, J. P., Schiebel, E., Driessen, A. J., and Wickner, W. (1990) The purified *E.*
400 *coli* integral membrane protein SecYE is sufficient for reconstitution of SecA-dependent
401 precursor protein translocation. *Cell* **62**, 649-657
- 402 6. Costello, S. M., Plummer, A. M., Fleming, P. J., and Fleming, K. G. (2016) Dynamic periplasmic
403 chaperone reservoir facilitates biogenesis of outer membrane proteins. *Proceedings of the*
404 *National Academy of Sciences* **113**, E4794-E4800
- 405 7. Li, G., He, C., Bu, P., Bi, H., Pan, S., Sun, R., and Zhao, X. S. (2018) Single-molecule detection
406 reveals different roles of Skp and SurA as chaperones. *ACS chemical biology* **13**, 1082-1089
- 407 8. Wu, S., Ge, X., Lv, Z., Zhi, Z., Chang, Z., and Zhao, X. S. (2011) Interaction between bacterial outer
408 membrane proteins and periplasmic quality control factors: a kinetic partitioning mechanism.
409 *Biochemical Journal* **438**, 505-511
- 410 9. Calabrese, A. N., Schiffrin, B., Watson, M., Karamanos, T. K., Walko, M., Humes, J. R., Horne, J. E.,
411 White, P., Wilson, A. J., and Kalli, A. C. (2020) Inter-domain dynamics in the chaperone SurA and
412 multi-site binding to its outer membrane protein clients. *Nature communications* **11**, 1-16
- 413 10. Gessmann, D., Chung, Y. H., Danoff, E. J., Plummer, A. M., Sandlin, C. W., Zaccari, N. R., and
414 Fleming, K. G. (2014) Outer membrane β -barrel protein folding is physically controlled by
415 periplasmic lipid head groups and BamA. *Proceedings of the National Academy of Sciences* **111**,
416 5878-5883
- 417 11. Doyle, M. T., and Bernstein, H. D. (2019) Bacterial outer membrane proteins assemble via
418 asymmetric interactions with the BamA β -barrel. *Nature communications* **10**, 1-13
- 419 12. Doyle, M. T., Jimah, J. R., Dowdy, T., Ohlemacher, S. I., Larion, M., Hinshaw, J. E., and Bernstein,
420 H. D. (2022) Cryo-EM structures reveal multiple stages of bacterial outer membrane protein
421 folding. *Cell* **185**, 1143-1156. e11113

- 422 13. Malinverni, J. C., Werner, J., Kim, S., Sklar, J. G., Kahne, D., Misra, R., and Silhavy, T. J. (2006) YfiO
423 stabilizes the YaeT complex and is essential for outer membrane protein assembly in *Escherichia*
424 *coli*. *Molecular microbiology* **61**, 151-164
- 425 14. Noinaj, N., Gumbart, J. C., and Buchanan, S. K. (2017) The β -barrel assembly machinery in
426 motion. *Nature Reviews Microbiology* **15**, 197-204
- 427 15. Williams, D. C., Van Frank, R. M., Muth, W. L., and Burnett, J. P. (1982) Cytoplasmic inclusion
428 bodies in *Escherichia coli* producing biosynthetic human insulin proteins. *Science* **215**, 687-689
- 429 16. Rogl, H., Kosemund, K., Kühlbrandt, W., and Collinson, I. (1998) Refolding of *Escherichia coli*
430 produced membrane protein inclusion bodies immobilised by nickel chelating chromatography.
431 *FEBS letters* **432**, 21-26
- 432 17. Schwarzer, T. S., Hermann, M., Krishnan, S., Simmel, F. C., and Castiglione, K. (2017) Preparative
433 refolding of small monomeric outer membrane proteins. *Protein expression and purification*
434 **132**, 171-181
- 435 18. Shanmugavadivu, B., Apell, H.-J., Meins, T., Zeth, K., and Kleinschmidt, J. H. (2007) Correct
436 Folding of the β -Barrel of the Human Membrane Protein VDAC Requires a Lipid Bilayer. *Journal*
437 *of Molecular Biology* **368**, 66-78
- 438 19. Surrey, T., and Jähnig, F. (1995) Kinetics of Folding and Membrane Insertion of a β -Barrel
439 Membrane Protein. *Journal of Biological Chemistry* **270**, 28199-28203
- 440 20. Kleinschmidt, J. H., and Tamm, L. K. (2002) Secondary and tertiary structure formation of the β -
441 barrel membrane protein OmpA is synchronized and depends on membrane thickness. *Journal*
442 *of molecular biology* **324**, 319-330
- 443 21. Burgess, N. K., Dao, T. P., Stanley, A. M., and Fleming, K. G. (2008) β -barrel proteins that reside
444 in the *Escherichia coli* outer membrane in vivo demonstrate varied folding behavior in vitro.
445 *Journal of Biological Chemistry* **283**, 26748-26758
- 446 22. Maurya, S. R., Chaturvedi, D., and Mahalakshmi, R. (2013) Modulating lipid dynamics and
447 membrane fluidity to drive rapid folding of a transmembrane barrel. *Scientific Reports* **3**, 1-6
- 448 23. Pocanschi, C. L., Apell, H.-J., Puntervoll, P., Høgh, B., Jensen, H. B., Welte, W., and Kleinschmidt,
449 J. H. (2006) The major outer membrane protein of *Fusobacterium nucleatum* (FomA) folds and
450 inserts into lipid bilayers via parallel folding pathways. *Journal of molecular biology* **355**, 548-561
- 451 24. Stetsenko, A., and Guskov, A. (2017) An overview of the top ten detergents used for membrane
452 protein crystallization. *Crystals* **7**, 197
- 453 25. Hong, H., Patel, D. R., Tamm, L. K., and van den Berg, B. (2006) The outer membrane protein
454 OmpW forms an eight-stranded β -barrel with a hydrophobic channel. *Journal of biological*
455 *chemistry* **281**, 7568-7577
- 456 26. Gupta, A., and Mahalakshmi, R. (2020) Single-residue physicochemical characteristics kinetically
457 partition membrane protein self-assembly and aggregation. *Journal of Biological Chemistry* **295**,
458 1181-1194
- 459 27. van den Berg, B. (2010) Crystal structure of a full-length autotransporter. *Journal of molecular*
460 *biology* **396**, 627-633
- 461 28. Van Den Berg, B., Black, P. N., Clemons, W. M., and Rapoport, T. A. (2004) Crystal structure of
462 the long-chain fatty acid transporter FadL. *Science* **304**, 1506-1509
- 463 29. Morgado, L., Zeth, K., Burmann, B. M., Maier, T., and Hiller, S. (2015) Characterization of the
464 insertase BamA in three different membrane mimetics by solution NMR spectroscopy. *Journal of*
465 *biomolecular NMR* **61**, 333-345
- 466 30. Balasubramaniam, D., Arockiasamy, A., Kumar, P., Sharma, A., and Krishnaswamy, S. (2012)
467 Asymmetric pore occupancy in crystal structure of OmpF porin from *Salmonella typhi*. *Journal of*
468 *structural biology* **178**, 233-244

- 469 31. Budiardjo, S. J., Ikujuni, A. P., Firlar, E., Cordova, A., Kaelber, J. T., and Slusky, J. S. (2021) High-
470 Yield Preparation of Outer Membrane Protein Efflux Pumps by in Vitro Refolding is
471 Concentration Dependent. *The Journal of Membrane Biology* **254**, 41-50
- 472 32. Bleuel, C., Große, C., Taudte, N., Scherer, J., Wesenberg, D., Krauß, G. J., Nies, D. H., and Grass,
473 G. (2005) TolC is involved in enterobactin efflux across the outer membrane of *Escherichia coli*.
474 *Journal of bacteriology* **187**, 6701-6707
- 475 33. Fralick, J. A. (1996) Evidence that TolC is required for functioning of the Mar/AcrAB efflux pump
476 of *Escherichia coli*. *Journal of bacteriology* **178**, 5803-5805
- 477 34. Nikaido, H. (2009) Multidrug resistance in bacteria. *Annual review of biochemistry* **78**, 119-146
- 478 35. Daury, L., Orange, F., Taveau, J.-C., Verchère, A., Monlezun, L., Gounou, C., Marreddy, R. K.,
479 Picard, M., Broutin, I., and Pos, K. M. (2016) Tripartite assembly of RND multidrug efflux pumps.
480 *Nature communications* **7**, 1-8
- 481 36. Swick, M. C., Morgan-Linnell, S. K., Carlson, K. M., and Zechiedrich, L. (2011) Expression of
482 multidrug efflux pump genes *acrAB-tolC*, *mdfA*, and *norE* in *Escherichia coli* clinical isolates as a
483 function of fluoroquinolone and multidrug resistance. *Antimicrobial agents and chemotherapy*
484 **55**, 921-924
- 485 37. Pradel, E., and Pagès, J.-M. (2002) The AcrAB-TolC efflux pump contributes to multidrug
486 resistance in the nosocomial pathogen *Enterobacter aerogenes*. *Antimicrobial agents and*
487 *chemotherapy* **46**, 2640-2643
- 488 38. Baucheron, S., Tyler, S., Boyd, D., Mulvey, M. R., Chaslus-Dancla, E., and Cloeckert, A. (2004)
489 AcrAB-TolC directs efflux-mediated multidrug resistance in *Salmonella enterica* serovar
490 Typhimurium DT104. *Antimicrobial agents and chemotherapy* **48**, 3729-3735
- 491 39. Sonoda, Y., Newstead, S., Hu, N.-J., Alguel, Y., Nji, E., Beis, K., Yashiro, S., Lee, C., Leung, J., and
492 Cameron, A. D. (2011) Benchmarking membrane protein detergent stability for improving
493 throughput of high-resolution X-ray structures. *Structure* **19**, 17-25
- 494 40. Masi, M., Duret, G., Delcour, A. H., and Misra, R. (2009) Folding and trimerization of signal
495 sequence-less mature TolC in the cytoplasm of *Escherichia coli*. *Microbiology* **155**, 1847
- 496 41. Krishnamoorthy, G., Tikhonova, E. B., Dhamdhare, G., and Zgurskaya, H. I. (2013) On the role of
497 TolC in multidrug efflux: the function and assembly of AcrAB-TolC tolerate significant depletion
498 of intracellular TolC protein. *Molecular microbiology* **87**, 982-997
- 499 42. Zakharov, S. D., Wang, X. S., and Cramer, W. A. (2016) The colicin E1 TolC-binding conformer:
500 pillar or pore function of TolC in colicin import? *Biochemistry* **55**, 5084-5094
- 501 43. Micsonai, A., Wien, F., Bulyáki, É., Kun, J., Moussong, É., Lee, Y.-H., Goto, Y., Réfrégiers, M., and
502 Kardos, J. (2018) BeStSel: a web server for accurate protein secondary structure prediction and
503 fold recognition from the circular dichroism spectra. *Nucleic acids research* **46**, W315-W322
- 504 44. Werner, J., Augustus, A. M., and Misra, R. (2003) Assembly of TolC, a Structurally Unique and
505 Multifunctional Outer Membrane Protein of *Escherichia coli* K-12. *Journal of Bacteriology* **185**,
506 6540-6547
- 507 45. Koronakis, V., Li, J., Koronakis, E., and Stauffer, K. (1997) Structure of TolC, the outer membrane
508 component of the bacterial type I efflux system, derived from two-dimensional crystals.
509 *Molecular microbiology* **23**, 617-626
- 510 46. German, G. J., and Misra, R. (2001) The TolC protein of *Escherichia coli* serves as a cell-surface
511 receptor for the newly characterized TLS bacteriophage. *Journal of molecular biology* **308**, 579-
512 585
- 513 47. Budiardjo, S. J., Stevens, J. J., Calkins, A. L., Ikujuni, A. P., Wimalasena, V. K., Firlar, E., Case, D. A.,
514 Biteen, J. S., Kaelber, J. T., and Slusky, J. S. G. (2022) Colicin E1 opens its hinge to plug TolC. *Elife*
515 **11**

- 516 48. Pei, X.-Y., Hinchliffe, P., Symmons, M. F., Koronakis, E., Benz, R., Hughes, C., and Koronakis, V.
517 (2011) Structures of sequential open states in a symmetrical opening transition of the TolC exit
518 duct. *Proceedings of the National Academy of Sciences* **108**, 2112-2117
- 519 49. Fitzpatrick, A. W., Llabrés, S., Neuberger, A., Blaza, J. N., Bai, X.-c., Okada, U., Murakami, S., Van
520 Veen, H. W., Zachariae, U., and Scheres, S. H. (2017) Structure of the MacAB–TolC ABC-type
521 tripartite multidrug efflux pump. *Nature microbiology* **2**, 1-8
- 522 50. Danoff, E. J., and Fleming, K. G. (2017) Novel kinetic intermediates populated along the folding
523 pathway of the transmembrane β -barrel OmpA. *Biochemistry* **56**, 47-60
- 524 51. Mitchell, D. J., Tiddy, G. J. T., Waring, L., Bostock, T., and McDonald, M. P. (1983) Phase
525 behaviour of polyoxyethylene surfactants with water. Mesophase structures and partial
526 miscibility (cloud points). *Journal of the Chemical Society, Faraday Transactions 1: Physical
527 Chemistry in Condensed Phases* **79**, 975-1000
- 528 52. Michael Garavito, R., and Rosenbusch, J. P. (1986) [25] Isolation and crystallization of bacterial
529 porin. in *Methods in enzymology*, Academic Press. pp 309-328
- 530 53. Boyd, B. J., Drummond, C. J., Krodziewska, I., and Grieser, F. (2000) How Chain Length,
531 Headgroup Polymerization, and Anomeric Configuration Govern the Thermotropic and Lyotropic
532 Liquid Crystalline Phase Behavior and the Air–Water Interfacial Adsorption of Glucose-Based
533 Surfactants. *Langmuir* **16**, 7359-7367
- 534 54. Raetz, C., and Dowhan, W. (1990) Biosynthesis and function of phospholipids in Escherichia coli.
535 *Journal of Biological Chemistry* **265**, 1235-1238

536

537

538 Supporting Information

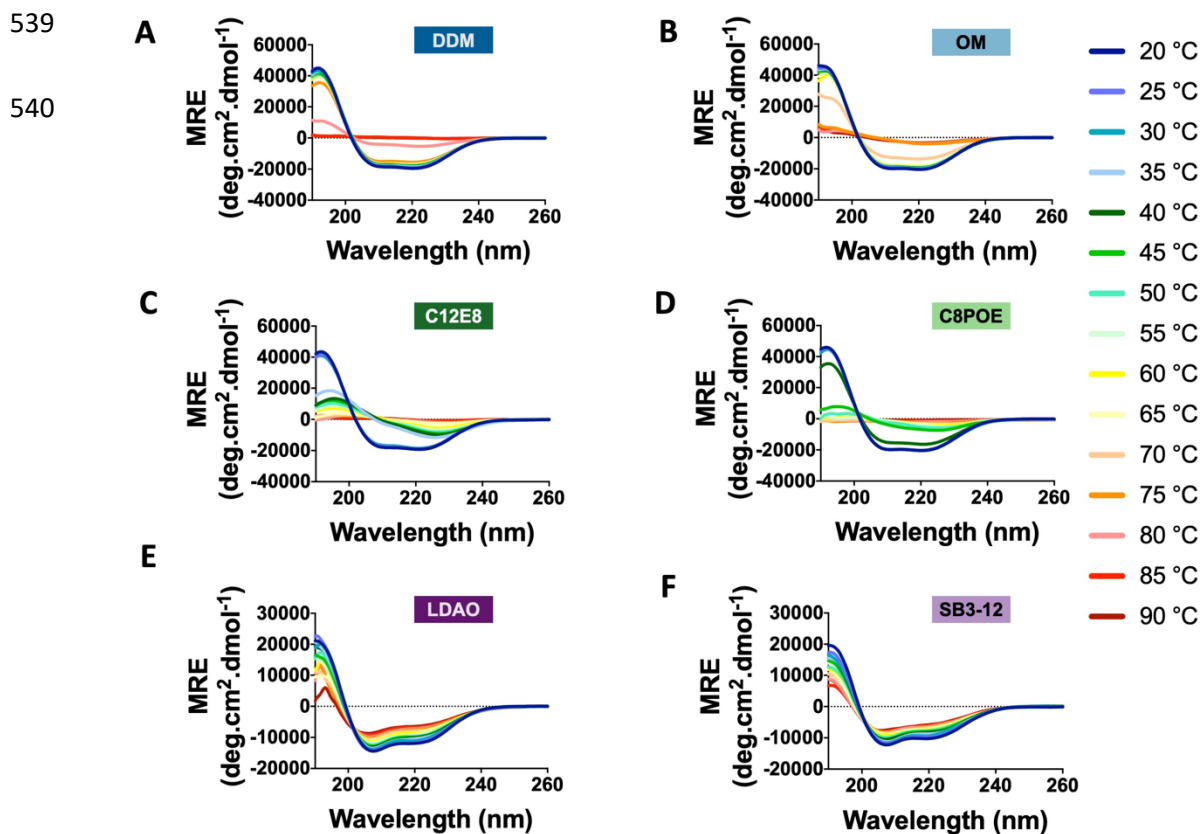


Figure S1: Thermal spectra of ToIC refolded in detergents. Change in circular dichroism spectrum per 5 °C increase in temperature from 20 °C to 90 °C of ToIC with alpha-helical intermediates in A and B and beta-sheet intermediates in C and D refolded in (A) DDM, (B) OM, (C) C12E8, (D) C8POE, (E) LDAO, and (F) SB3-12.